SCIENTIFIC REPORTS

OPEN

High thermopower of mechanically stretched single-molecule junctions

Received: 17 November 2014
Accepted: 29 May 2015
Published: 26 June 2015

Makusu Tsutsui, Takanori Morikawa, Yuhui He, Akihide Arima & Masateru Taniguchi

Metal-molecule-metal junction is a promising candidate for thermoelectric applications that utilizes quantum confinement effects in the chemically defined zero-dimensional atomic structure to achieve enhanced dimensionless figure of merit *ZT*. A key issue in this new class of thermoelectric nanomaterials is to clarify the sensitivity of thermoelectricity on the molecular junction configurations. Here we report simultaneous measurements of the thermoelectric voltage and conductance on Au-1,4-benzenedithiol (BDT)-Au junctions mechanically-stretched *in-situ* at sub-nanoscale. We obtained the average single-molecule conductance and thermopower of 0.01 G_0 and 15 μV/K, respectively, suggesting charge transport through the highest occupied molecular orbital. Meanwhile, we found the single-molecule thermoelectric transport properties extremely-sensitive to the BDT bridge configurations, whereby manifesting the importance to design the electrode-molecule contact motifs for optimizing the thermoelectric performance of molecular junctions.

Electron transport in an organic molecule connected to metal leads has been extensively explored for applications in nanosensors and nanoelectronics[1–4] In this virtually zero-dimensional nanostructure, simultaneous enhancement of electrical conductance and thermopower can be achieved by exploiting the steep peak in the density of states at the frontier molecular orbital levels, thereby opening new perspectives for achieving high thermoelectric figure of merit[5,6] Owing to the advance in single-molecule technologies, it has become increasingly feasible to experimentally address the thermoelectric transport in individual molecular wires[7–10] Despite the progress, however, while it is well-established that the single-molecule conductance varies widely depending on the molecular conformations and the electrode-molecule contact structures, little is known about the thermopower sensitivity on the molecular junction configurations, which is of fundamental importance for the development of efficient molecular thermoelectric devices[11,12] In fact, geometry-sensitive nature of Seebeck coefficient was found in nanosystems similar to molecular junctions such as metal atom-sized contacts[13,14].

Here we demonstrate statistical evaluation of geometric effects on the thermoelectric transport in 1,4-benzenedithiols (BDTs) anchored to Au nanoelectrodes at the single-molecule level. Au-BDT-Au bridge is known to possess a broad range of electric conductance due to the geometry-sensitive electronic coupling strength at the electrode-molecule links[15–17], and therefore serves as a suitable model system for examining the structural dependence of thermoelectricity in a single-molecule wire.

Results

Simultaneous measurements of single-molecule conductance and thermoelectric voltage. A microheater-embedded mechanically-controllable break junction (MCBJ)[18] was used to investigate the thermoelectric transport in Au-BDT-Au structures (Fig. 1a). In this device, a molecular-sized electrode gap can be formed by breaking Au nanobridge through mechanical deflection of the substrate. Then, BDT interconnects the nanoelectrodes whereby form a Au-BDT-Au junction. The ability to finely adjust the electrode positions enabled formation of many molecular bridges with different configurations in a

The Institute of Scientific and Industrial Research, Osaka University, 8-1 Mihogaoka, Ibaraki, Osaka 567-0047, Japan. Correspondence and requests for materials should be addressed to M.T. (email: tsutsui@sanken.osaka-u.ac.jp)

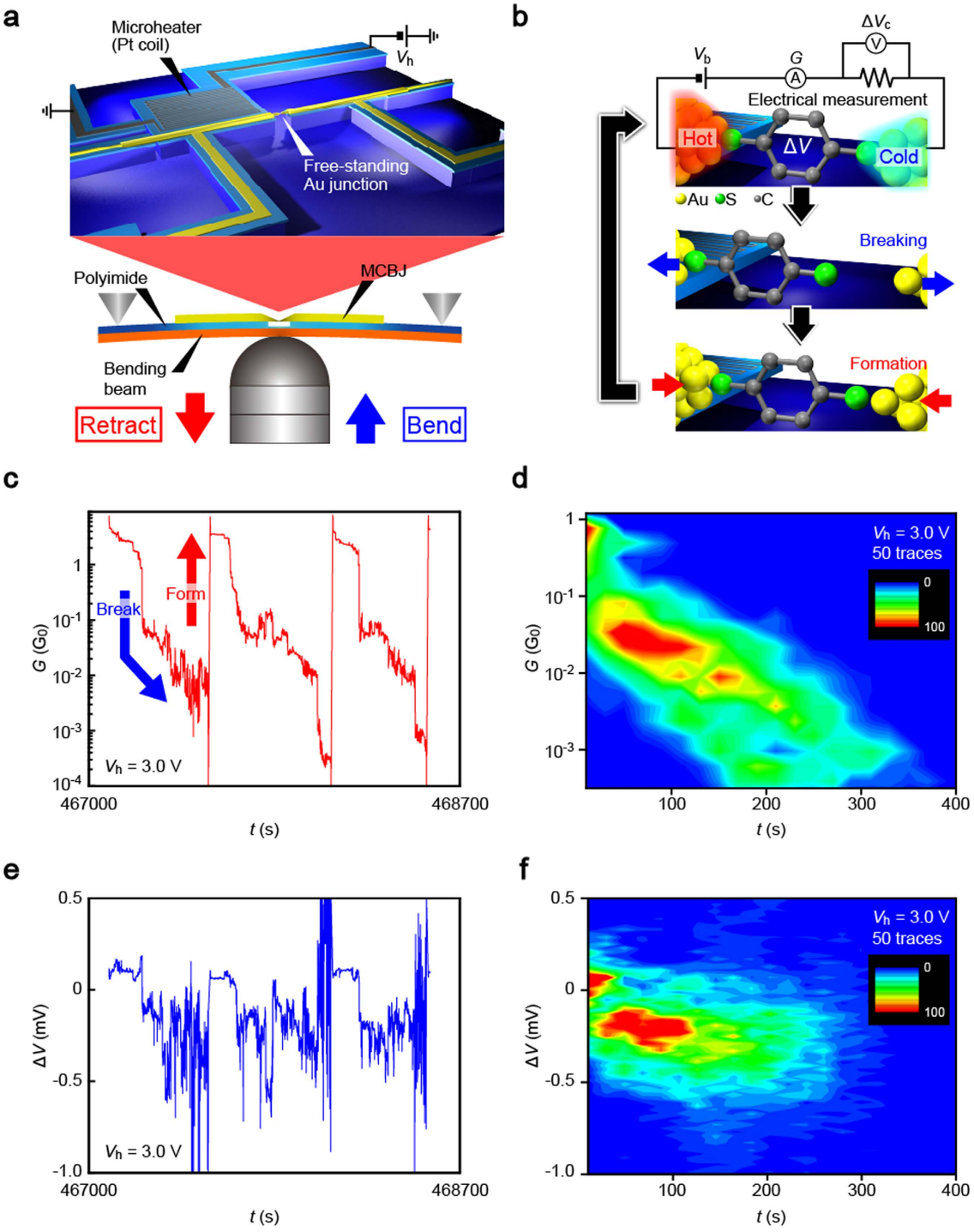

Figure 1. Simultaneous measurements of conductance and thermoelectric voltage of molecular junctions. (**a**), A microheater-embedded mechanically-controllable break junction used for forming stable Au-BDT-Au junctions at room temperatures. The free-standing Au junction was broken and reformed through manipulating the substrate bending via piezo-control. The adjacent Pt microheater was heated under the applied voltage V_h to create a temperature gradient at the junction for inducing detectable level of thermovoltage. (**b**), Schematic description of the measurement scheme. The conductance of molecular junctions was obtained by recording current under dc voltage $V_b = 0.2$ V. Subsequently, the potential drop at the 100 kΩ sensing resistor ΔV_c was acquired at $V_b = 0$ V, from which the thermovoltage at the junction ΔV was deduced. The sequential G - ΔV_c measurements were performed in the course of repeated formation and breaking of BDT molecular junctions. **c-d,** Partial $G - t$ curve (**c**) and corresponding two-dimensional histogram (**d**) obtained at $V_h = 3.0$ V. **e-f,** The simultaneously recorded $\Delta V - t$ trace (**e**) and the two-dimensional histogram (**f**).

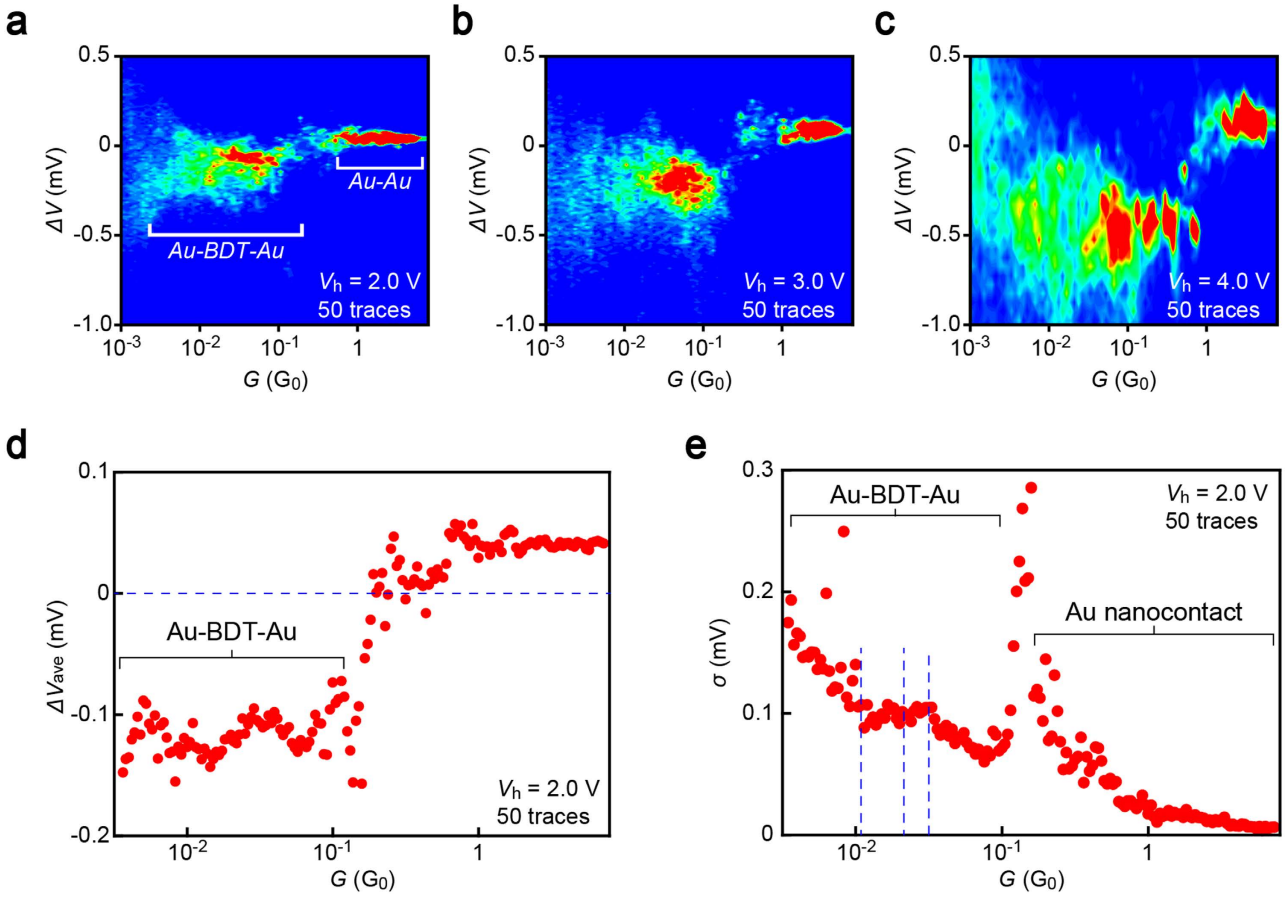

Figure 2. Single-molecule conductance versus thermoelectric voltage characteristics. a-c, $\Delta V - G$ diagrams of BDT junctions at $V_h = 2.0$ V (**a**), 3.0 V (**b**), and 4.0 V (**c**). **d,** ΔV_{ave} versus G semilog plots at $V_h = 2.0$ V. Dashed line denote $\Delta V_{ave} = 0$ V. **e,** The standard deviation σ in ΔV plotted against G. Dashed lines represent $G = nG_{BDT}$ for $n = 1$ to 3, where $G_{BDT} = 0.011\ G_0$ is the single-molecule conductance of Au-BDT-Au junctions. A sharp rise in σ at $G \sim 0.2\ G_0$ signifies a transition between Au atomic wires and BDT molecular junctions during the break junction experiments whereat the thermoelectric voltage changes its sign from positive to negative (see also Fig. S8).

short time allowing characterization of a variation in the thermoelectric transport in the molecular wires by utilizing the microheater to create a temperature gradient for inducing thermoelectric voltage there (Fig. 1b)[14,19]

The conductance G and thermoelectric voltage ΔV were simultaneously measured during stretching of BDT-decorated Au junctions (Figs S1-S2). We observed stepwise decrease in G as the Au nanocontact was narrowed by tensile deformation. Eventually, the junction was shrunk to one-atom size, which was confirmed by observations of long plateaus at 1 G_0, where $G_0 = 2e^2/h$ is the conductance quantum the electron mass e and Plank constant h. After breakage of the single-atom contacts, G dropped rapidly and showed another plateaus often with negative slope in a conductance range from 10^{-1} to $10^{-4}\ G_0$ (Fig. 1c). Conductance histograms revealed broad distributions but with several pronounced peaks at $n \times G_{BDT}$ ($n = 1, 2, 3$) with $G_{BDT} = 0.011\ G_0$ in accordance with the single-molecule conductance for Au-BDT-Au junctions reported in previous literatures[15–17] (Fig. S5). The overall tendency can be also found in the two-dimensional histogram (Fig. 1d) where data are clustered at around $10^{-2}\ G_0$ corresponding to single- or a few BDT molecules bridging the Au nanoelectrodes[20–22] On the other hand, the thermoelectric voltage showed fluctuations at around a certain value upon formations of the molecular junctions until G dropped to zero (Figs 1e-f and S6).

Thermovoltage-conductance diagrams. Geometrical dependence of thermoelectricity in molecular junctions is investigated by constructing $G - \Delta V$ diagrams (Figs 2 and S7). The negative thermoelectric voltage of BDT molecular junctions tend to become higher with increasing heater voltage due to the larger temperature gradient created under elevated V_h (Fig. 2a–c). The average thermoelectric voltage ΔV_{ave} was found to change little over two orders of magnitude difference in G in the entire V_h range

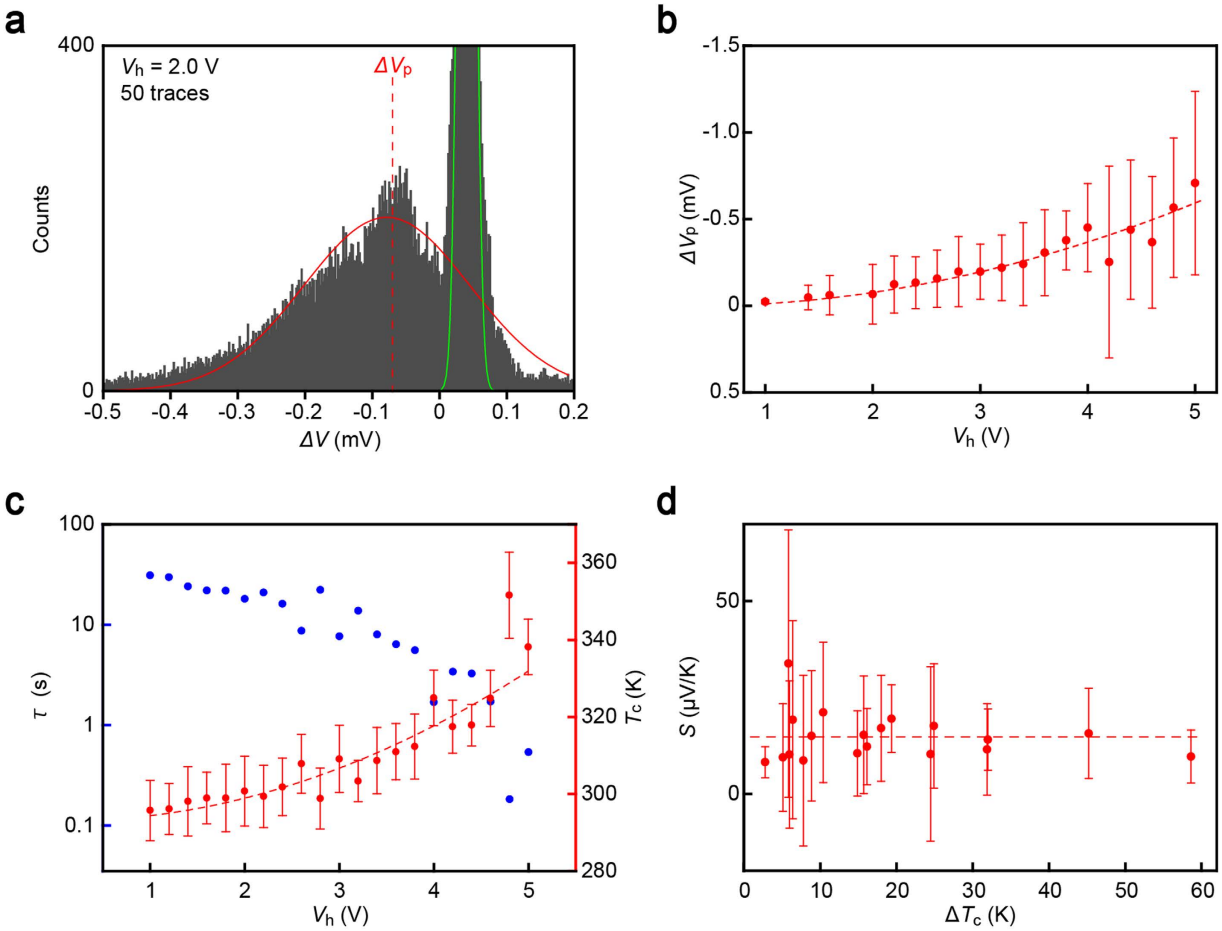

Figure 3. Single-molecule thermopower. a, Histogram of ΔV at $V_h = 2.0$ V. Peaks at the positive and negative regimes correspond to the thermovoltage occurred at Au atom-sized contacts and BDT molecular junctions, respectively. Red solid curve is Gaussian fitting to the thermoelectric voltage distribution that define the peak voltage ΔV_p for BDT single molecule junctions. Green curve is the fit to the thermovoltage distribution for Au contacts. **b,** Heater voltage dependence of ΔV_p. The negative values reflect the thermoelectric characteristics of BDT junctions. Dashed lines are V_h^2 fits. Error bars denote the full-width at half-maximum of the V_p distributions. **c,** Au single-atom contact lifetime τ (blue) and the estimated local contact temperature T_c (red) plotted with respect to V_h. Dashed line is a quadratic fit to T_c. **d,** Thermopower S of BDT molecular junctions plotted against ΔT_c. Dashed lines are the average of S.

measured (Figs 2d and S8). This interesting feature would be interpreted by attributing the broad-range conductance to a formation of parallel circuits consisting of n BDTs with conductance G_{BDT}, as the resulting thermoelectric voltage is essentially independent of the number of current-carrying molecules[7]. If this is the case, however, fluctuations in ΔV should become smaller at higher G since the measured thermovoltage would tend to be averaged by the number of molecules[10], which is not consistent with that the standard deviation σ of ΔV changes little with G (Figs 2e and S10). The conductance-insensitive manner of the average thermoelectric voltage seems to be, therefore, an intrinsic property of BDT single-molecule wires.

Average thermopower of BDT single-molecule junctions. To shed further light on the thermoelectric effects in Au-BDT-Au tunnelling junctions, we deduced the thermopower S from V_h-dependence of the thermoelectric voltage. ΔV histograms show bimodal distribution (Fig. 3a). The broad feature at the negative region denote the expansive variation in ΔV of the BDT bridges. We extracted the peak values ΔV_p from each ΔV histogram, which demonstrate the typical thermoelectric characteristic of the molecular junctions, at various heater voltage conditions. $\Delta V_p - V_h$ correlation reveal steady increase in the average thermoelectric voltage with the heater voltage (Fig. 3b).

Derivation of single-molecule thermopower requires the temperature gradient ΔT_c at the junction. For this, we used the lifetime τ of Au atomic wires as an indirect thermometer to estimate the local temperature T_c at the vicinity of junctions[21,23] τ was obtained from the plateau length within a conductance

window of 0.8 G_0 to 1.2 G_0 in the G - t curves (Fig. S13), from which V_h-dependence of T_c was assessed using Arrhenius expression $\tau = f_0^{-1}\exp(E_B/k_BT_c)$, where $f_0 = 3 \times 10^{12}$ Hz, E_B, and k_B denote the attempt frequency, the critical bond strength in the contact, and Boltzmann factor, respectively (Fig. 3c)[18,24,25] Specifically, we performed linear fitting in the $\ln\tau$ versus V_h^2 plots and deduced E_B from the fact that $T_c = 293$ K when $V_h = 0$ V. As a result, we obtained $E_B = 0.82$ eV. This value is slightly higher than the typical Au-Au bond energy in the single-atom chain[24], which is attributable to enhancement of the contact stability via the dithiol molecules bridged in parallel[26,27]. Eventually, we acquired $\Delta T_c = T_c - T_0$ assuming that one side of the junction was kept at ambient temperatures $T_0 = 293$ K (Fig. S3)[7] and calculated the average thermopower of BDT single-molecule junctions through $S = -\Delta V_p/\Delta T_c$. We obtained positive thermopower of $S_{BDT} = 15 \pm 4\,\mu$V/K, the sign of which confirms dominant charge transport mechanisms in the two systems: hole tunnelling through the highest occupied molecular orbital (HOMO) level in the Au-BDT-Au system. Moreover, the present thermopower value is in good quantitative agreement with the previous experiment on many-molecule junctions[7], which in turn indicates that the thermoelectric power of molecular junctions changes little with the number of constituent molecules. Note that S_{BDT} is a lower limit value as the temperature at the heat downstream of BDT junctions may be heated to above 293 K (Fig. S3).

Single-molecule thermopower sensitivity on mechanical stretching. The above results imply moderate impact of configurational degree of freedom on the thermoelectric effects in BDT junctions as a whole. However, it does not necessarily mean that there is no geometrical dependence; in sharp contrast, we often detected subtle change in the thermovoltage during mechanical stretching of Au-BDT-Au junctions in the respective traces (Fig. 4a). The electromechanical response could be classified into three groups: steady thermopower rise (TR) or decrease (TD) and rapid rise in ΔV entailing concomitant enhancement in G (RI) before the junction breakdown (Figs 4b and S13). It is noticeable that the conductance exhibits a steady decrease irrespective of the types of $\Delta V - t$ characteristics. This corroborates the predominant influence of molecule-electrode coupling on charge transmission probability in BDT junctions[15,16,28], which on the other hand causes only minor effects on the thermoelectric power thereby giving rise to the G-independent behavior of ΔV_{ave}[28,29].

From practical viewpoints, the configurations achieved in RI events are a superior design of Au-BDT-Au junctions that realize two orders of magnitude improvement in the power factor S^2G from the average value $S_{BDT}{}^2G_{BDT}$ through concurrent enhancement of ΔV and G. In an optimal case (Figs. 4c and S13), we observed $S_{BDT} = 120\,\mu$V/K and $G_{BDT} = 0.21\ G_0$. This particular BDT bridge attains a high power factor of 0.25 pW/K^2 that is three orders of magnitude higher than 0.19 fW/K^2 calculated from $S_{BDT} = 15\,\mu$V/K and $G_{BDT} = 0.011\ G_0$ of the average junctions. The present work thus suggests the importance of engineering not only the molecular structure but also the atomic junction configurations for pursuing high-performance single-molecule thermoelectrics.

Discussion

It is intriguing that the average thermopower of BDT single-molecule junctions changes little over the broad range of the conductance. In bulk materials, the thermopower is described by the Mott's theory that states $S \sim (\partial N(E)/\partial E|_{E=E_F})/N(E_F)$, where $N(E)$ and E_F is the density of states at the energy E and the Fermi level, respectively[30]. This generally leads to a tradeoff between G and S as an improvement in the conductivity by increased $N(E_F)$ will be compensated by accompanying diminishment in the thermopower. The tunability of the single-molecule thermopower independently from the conductance may thus enable a unique way of engineering the thermoelectric properties of molecular junctions.

The S - G characteristics is interpreted by considering that HOMO of Au-BDT-Au junctions lies ~ 1 eV away from the electrode $_F$ermi level E_F[28]. The thermovoltage in the molecular tunnelling junctions is determined by the slope of transmission curves near E_F, *i.e.* $\Delta V \sim (\partial \ln T_i/\partial E|_{E=E_F})$, where T_i is the charge transmission[29]. On the other hand, the extensive range of G is anticipated to be stemming from a variation in the coupling strength at the left Γ_L and right Γ_R sides of the molecule-electrode contacts engendered by a stochastic nature in the contact mechanics[15,16]. While stronger coupling tends to broaden the transmission curve, the contribution on S is less significant for a metal-molecule-metal junction with a large E_F-HOMO energy gap E_{gap} (Fig. 5a)[28,29]. Hence, the constant average thermopower suggests reproducible formations of BDT single-molecule junctions with large E_{gap} but different degrees of $\Gamma_{L,R}$.

More quantitatively, when estimating E_{gap} and $\Gamma_{L,R}$ (BDTs are assumed to couple equally to both sides of Au electrodes) from the simplified Landauer expression of S_{BDT} and G_{BDT} in the weak coupling regime (i.e., $E_{gap} << \Gamma_{L,R}$),[31] we obtain $E_{gap} = 0.97$ eV and $\Gamma_{L,R} = 0.10$ eV for the typical BDT junctions with $S_{BDT} \sim 15\,\mu$V/K (Fig. 5a,b), which is in good agreement with the previous works[28,29] Compared to the average BDT bridges, the high-S single-molecule junction (Fig. 4d) possesses much smaller HOMO-E_F energy gap of 0.10 eV with weaker electronic coupling strength, $\Gamma_{L,R} = 0.05$ eV (Fig. 5b).

We note that recent experiments by Kim *et al.*[16] report narrower E_{gap} of about 0.3 eV, which is in good agreement with GW calculations[32]. Although this discrepancy may stem from the simple model we used, i.e. single-particle model with symmetric coupling, it is difficult to directly compare the energy gap we obtained with the value in the literature as the approaches for deriving the energy gap are quite different in the two works (thermopower or I-V) together with the temperature conditions used (above 300 K or

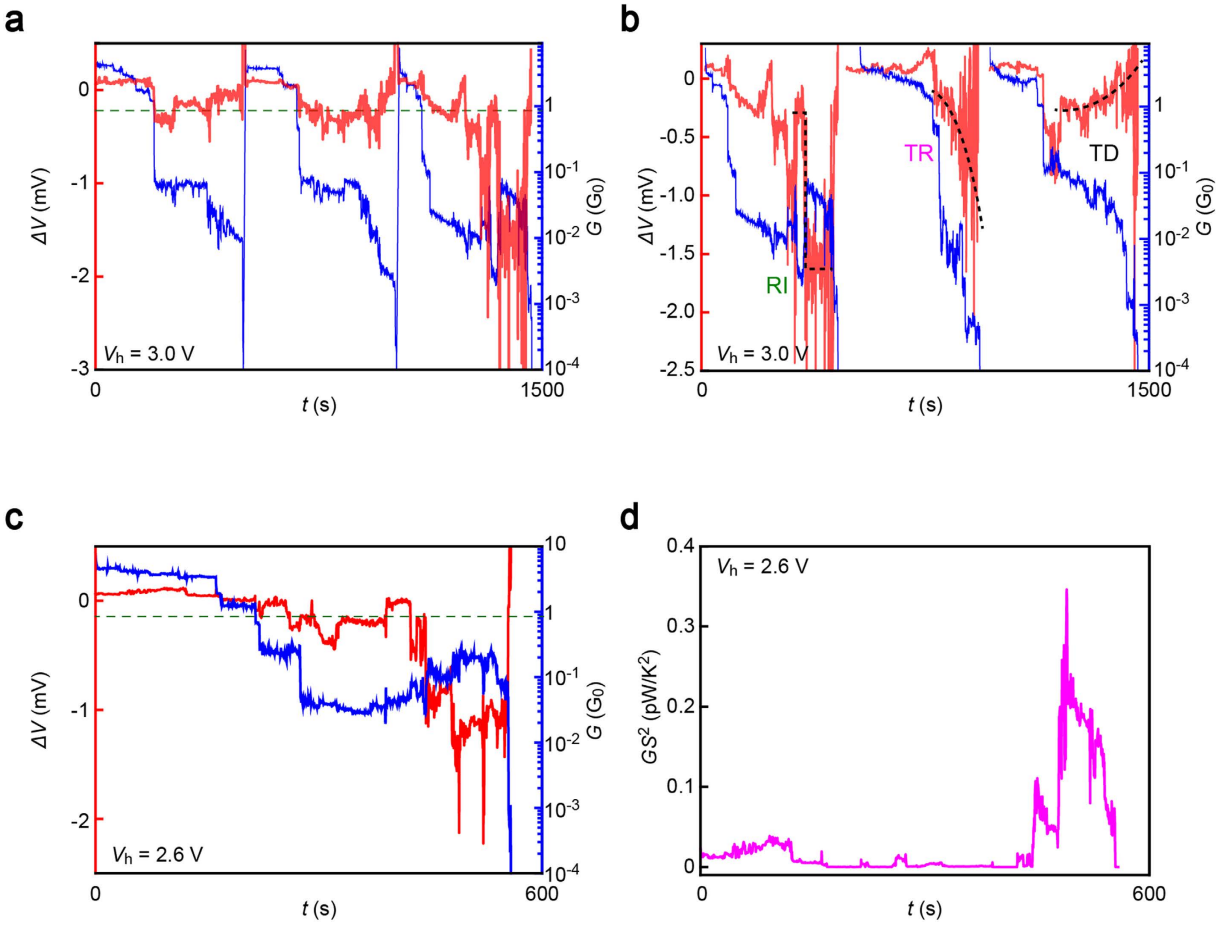

Figure 4. Mechanical response of thermovoltage. a, Three consecutive G (blue) and ΔV (red) traces at $V_h = 3.0$ V. Green dashed line indicates ΔV_{ave}. Whereas the first two junctions possessed ΔV close to the average value, the third junction show a high thermovoltage exceeding ΔV_{ave} by more than an order of magnitude. **b,** Three types of stretching dependence of ΔV (red) in BDT junctions demonstrating rapid increase (RI), steady rise (TR), and steady decrease (TD) in the absolute value of the thermoelectric voltage by junction elongation. The graph also displays the simultaneously recorded G (blue). **c,** BDT junction with optimal thermoelectric properties observed in the present work that possess $S_{BDT} = 120\,\mu$V/K and $G_{BDT} = 0.21\ G_0$ after RI. Red and blue curves denote the mechanical response of G and ΔV, respectively. **d,** Power factor GS^2 calculated from data in (**c**).

4.2 K) that should give rise to different contact mechanics and hence different junction geometries are quite different. Further effort should be thus devoted to address the quantitative accuracy of the analysis method described here.

The geometrical dependence of thermoelectricity in Au-BDT-Au junctions is inferred in the $\Delta V - t$ profiles. TR and TD tendencies clearly suggest accompanying roles of the mechanical stretching along specific directions, which results in molecular tilting toward an upright conformation and elongation of the Au-S bond lengths of BDT in a Au-hollow or -top geometry, to weaken the electrode-molecule electronic coupling that leads to steady decrease in G and meanwhile inducing gradual shift of HOMO toward or away from E_F, respectively[33–36]. On the other hand, the rapid increase in both G and ΔV of RI indicates a drastic change in the Fermi alignment: E_{gap} lowered for more than 0.5 eV and $\Gamma_{L,R}$ decreased by up to 0.05 eV. This anomalous feature presumably stems from over-elongated Au-S bonds of mechanically-stretched BDT junctions and accompanied electrode-to-thiol charge transfer that would provide additional MOs near E_F with weak electronic coupling, and hence small E_{gap} and $\Gamma_{L,R}$. It was in fact demonstrated theoretically that thermopower increases rapidly under stretching just before junction breakdown[36]. Furthermore, the fact that BDT junctions tended to dissociate in a relatively short period of time after the RI events infers the contact mechanics involved therein: unstable electrode-molecule link is formed at the Au-S contacts probably having an adatom-coordinated metastable motif with relatively long Au-S distance through pulling-out of the Au surface atoms during mechanical stretching[17,36] For this to happen, molecular junctions are required to endure the forces and thermal fluctuations until the

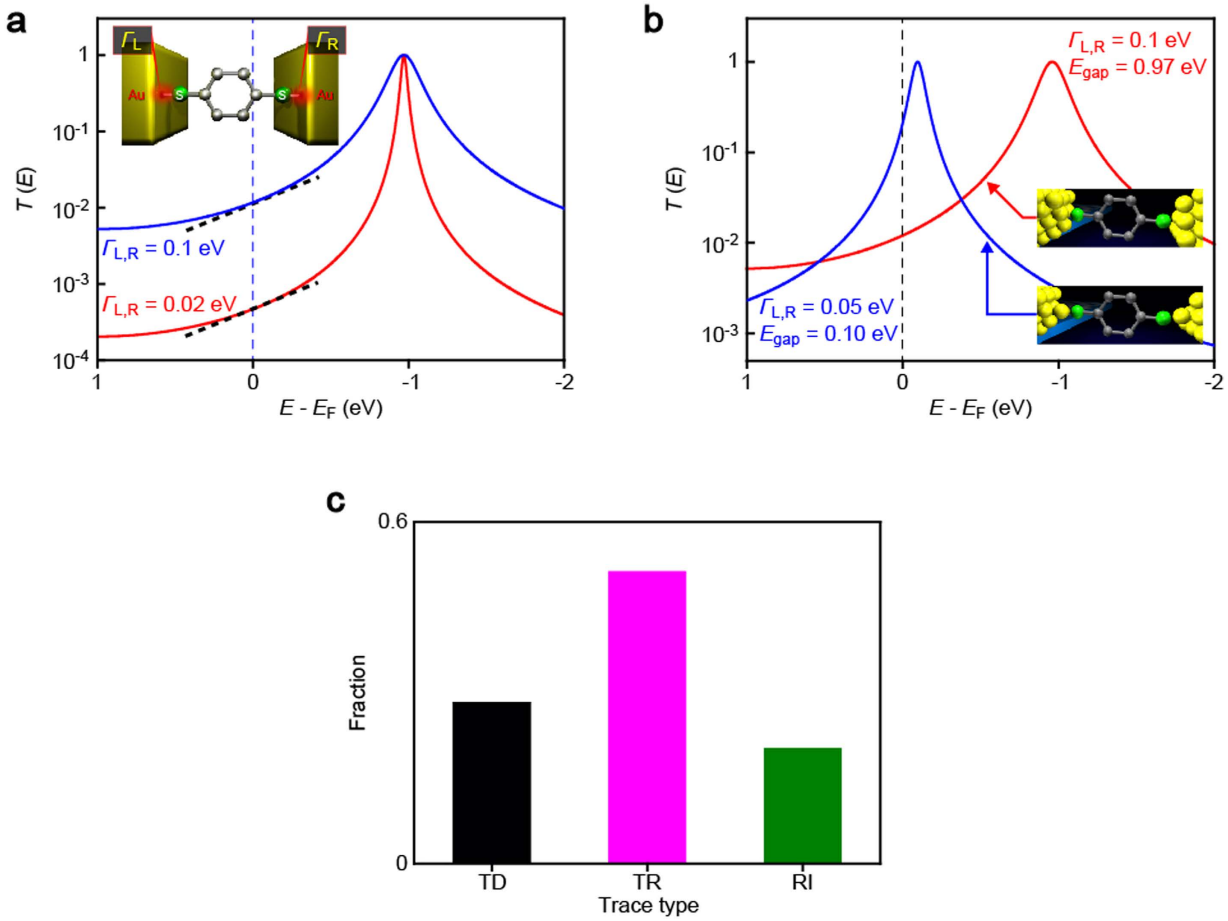

Figure 5. Geometrical dependence of thermoelectric voltage in single-molecule junctions. a, Coupling-insensitive thermopower of BDT tunnelling junctions. A transmission curve calculated for the average properties of $S_{BDT} = 15\,\mu V/K$ and $G_{BDT} = 0.011\ G_0$ (blue) using Lorentzian expression of the transmission $T(E) = \frac{8e^2\Gamma_L\Gamma_R}{h\left[(\Gamma_L+\Gamma_R)^2+4E_{gap}^2\right]}$ and the thermopower $S_{BDT} = \frac{8\pi^2k_B^2TE_{gap}}{3e\left[(\Gamma_L+\Gamma_R)^2+4E_{gap}^2\right]}$ with $E_F = 5.0\,eV$, where E_{gap} is the HOMO-Fermi level gap and $\Gamma_{L,R}$ is the coupling strength at the left and right electrodes. While the curve tends to become sharper under lower Γ (red), the slope of the transmission curve at the electrode Fermi level E_F (black dotted lines) changes little due to the relatively large E_{gap} of $E_{gap} = 0.97\,eV$. **b,** Transmission curve for BDT junctions having $E_{gap} = 0.10\,eV$ with $\Gamma_{L,R} = 0.05\,eV$ (blue) as deduced from $S_{BDT} = 120\,\mu V/K$ with $G_{BDT} = 0.21\ G_0$ attained by a specific junction displayed in Fig. 4c. A curve for the average junctions is also shown (red). The schematic models denote possible junction motifs responsible for the two different thermoelectric properties having a hollow-hollow geometry and an adatom-coordinated configuration. **c,** The normalized number of events for the three $\Delta V - t$ characteristics.

contact is departed at a certain extent, which is likely to be a rare case as Au-BDT-Au structure fractures spontaneously at the Au-Au contacts in vicinity of the Au-S link as illuminated by that the RI feature was found in only about 20 % of the traces measured (Fig. 5c). We expect that future works will shed more light on the physics underlies this intriguing effect found in the stretched molecular junctions.

Methods

Fabrication of heater-embedded MCBJs. A phosphor-bronze beam of 0.5 mm thickness was covered with a 4 μm thick polyimide layer. We then formed Au micro-leads on the polyimide using photolithography and radio-frequency magnetron sputtering processes followed by lift-off in *N*,*N*-dimethylformamide. After that, Al_2O_3 heat sinks were fabricated through delineating two island patterns by an electron-beam lithography with ZEP-520A-7 resist, subsequent inductively-coupled plasma sputtering for depositing a 40 nm thick Al_2O_3 layer, and the lift-off procedure. A Pt coil and a Au nano-junction were further prepared on the Al_2O_3 regions by the electron-beam processes and the sputtering. After the nanofabrications, the sample substrates were exposed to isotropic reactive ion etching with oxygen etchant gas for sculpting the polyimide. As a result, we obtained a free-standing Au junction of length approximately

2 μm. On the substrate, a Teflon ring was fixed on the substrate surface using polyimide as glue, which was used to fill in a molecular solution in prior to the break junction experiments. The cross-plane heat leakage was effectively suppressed by the thick polyimide layer that has excellent thermal insulating properties. Meanwhile, the Al_2O_3 layers served as effective thermal link to conduct the Joule heat at the Pt coil to the Au junction for generating finite temperature gradient to induce measureable thermoelectric voltage[16].

Formations of BDT single-molecule junctions. A Teflon ring cell on a MCBJ substrate was filled with a dilute toluene solution of BDT molecules adjusted to a concentration of 1 μM. Toluene and BDT were purchased from Aldrich Co. and utilized as-received. The MCBJ bending beam was then bent by a three-point bending mechanism to adhere BDT molecules on the fresh breakage Au surface. The chamber was then evacuated to remove the solvent while leaving BDTs strongly bound to the Au surface via Au-S bonds. When the vacuum reached below 10^{-5} Torr, we started the single-molecule measurements at room temperatures under various V_h conditions. In this, the BDT-decollated Au junction was broken and formed repeatedly in a controlled manner by manipulating the motion of a piezo-driven pushing rod (Fig. S1). At the same time, the temporal change in the junction conductance and the potential drop at the sensing resistor were monitored.

Thermoelectric voltage and electrical conductance measurements. The potential voltage drop at the sensing resistor ΔV_c and the junction conductance G were simultaneously recorded under constant V_h conditions when the junction conductance was below 8 G_0 in course of the break junction experiments. A picoammter/source unit (Keithley 6487) was used to obtain G under a dc voltage $V_b = 0.1$ V. After collecting G, V_b was set to 0 V and ΔV_c was measured by a nanovoltometer (Keithley 2182A). The measurement system and the motion of the piezo-element beading the MCBJ substrate were GPIB-controlled for automated measurements of many BDT single-molecule junctions under various V_h conditions (Fig. S2). Because of the small thermal current in the high-resistance molecular tunnelling junctions, which is on the order of pA, the integration time necessary for the nanovoltometer to acquire the thermoelectric voltage with accuracy exceeds 0.1 seconds. The overall measurement time to record G and ΔV_c was therefore as long as 0.3 seconds. Under this circumstance, a slow junction stretching rate of 6 pm/s was used to induce the mechanical deformations of Au-BDT-Au junctions, as it is critically important to preserve the junction status, including the molecule-electrode configurations and the molecular conformations, for prolong time to enable measurements of the thermopower and the electrical conductance for each molecular junctions with distinct geometries.

Data analysis. The junction conductance G was obtained by subtracting the 100 kΩ series resistance from the measured conductance. The actual thermoelectric voltage ΔV occurring at the junction was deduced from $\Delta V = \Delta V_c(1 + 10^{-5}/G)$ considering voltage division at the sensing resistor after background subtraction (Fig. S2). The background ΔV was calibrated at every measurement for each V_h condition by collecting G and ΔV_c at $V_h = 0$ V for 10 trials of the repeated junction formation/breaking processes in the beginning.

References

1. Lindsay, S. M. & Ratner, M. A. Molecular transport junctions: Clearing mists. *Adv. Mater.* **19,** 23–31 (2007).
2. Galperin, M., Ratner, M. A., Nitzan, A. & Troisi, A. Nuclear coupling and polarization in molecular transport junctions: Beyond tunnelling to function. *Science* **319,** 1056–1060 (2008).
3. Zwolak, M. & Di Ventra, M. Colloquium: Physical approaches to DNA sequencing and detection. *Rev. Mod. Phys.* **80,** 141–165 (2008).
4. Tsutsui, M. & Taniguchi, M. Single molecule electronics and devices. *Sensors* **12,** 7259–7298 (2012).
5. Dubi, Y. & Di Ventra, M. Colloquium: Heat flow and thermoelectricity in atomic and molecular junctions. *Rev. Mod. Phys.* **83,** 131–155 (2011).
6. Malen, J. A., Yee, S. K., Majumdar, A. & Segalman, R. A. Fundamentals of energy transport, energy conversion, and thermal properties in organic-inorganic heterojunctions. *Chem. Phys. Lett.* **491,** 109–122 (2010).
7. Reddy, P., Jang, S.–Y., Segalman, R. A. & Majumdar, A. Thermoelectricity in molecular junctions. *Science* **315,** 1568–1571 (2007).
8. Widawsky, J. R., Darancet, P., Neaton, J. B. & Venkataraman, L. Simultaneous determination of conductance and thermopower of single molecule junctions. *Nano Lett.* **12,** 354–358 (2011).
9. Evangeli, C. *et al.* Engineering the thermopower of C_{60} molecular junctions. *Nano Lett.* **13,** 2141–2145 (2013).
10. Guo, S., Zhou, G. & Tao, N. Single molecule conductance, thermopower, and transition voltage. *Nano Lett.* **13,** 4326–4332 (2013).
11. Malen, J. A., Doak, P., Baheti, K., Majumdar, A. & Segalman, R. A. The nature of transport variations in molecular heterojunction electronics. *Nano Lett.* **9,** 3406–3412 (2011).
12. Dubi, Y. Possible origin of thermoelectric response fluctuations in single-molecule junctions. *New J. Phys.* **15,** 105004 (2013).
13. Ludoph, B. & van Ruitenbeek, J. M. Thermopower of atomic-size metallic contacts. *Phys. Rev. B* **59,** 12290–12293 (1999).
14. Tsutsui, M., Morikawa, T., Arima, A. & Taniguchi, M. Thermoelectricity in atom-sized junctions at room temperatures. *Sci. Rep.* **3,** 3326 (2013).
15. Basch, H., Cohen, R. & Ratner, M. A. Interface geometry and molecular junction conductance: Geometric fluctuation and stochastic switching. *Nano Lett.* **5,** 1668–1675 (2005).
16. Kim, Y., Pietsch, T., Erbe, A., Belzig, W. & Scheer, E. Benzenedithiol: A broad-range single-channel molecular conductor. *Nano Lett.* **11,** 3734–3738 (2011).
17. Bruot, C. & Tao, N. Mechanically controlled molecular orbital alignment in single molecule junctions. *Nat. Nanotechnol.* **7,** 35–40 (2012).

18. Tsutsui, M., Kawai, T. & Taniguchi, M. Unsymmetrical hot electron heating in quasi-ballistic nanocontacts. *Sci. Rep*. **3,** 217 (2012).
19. Morikawa, T., Arima, A., Tsutsui, M. & Taniguchi, M. Thermoelectric voltage measurements of atomic and molecular wires using microheater-embedded mechanically-controllable break junctions. *Nanoscale* **6,** 8235–8241 (2014).
20. Xiao, X., Xu, B. & Tao, N. J. Measurement of single molecule conductance: Benzenedithiol and benzenedimethanethiol. *Nano Lett.* **4,** 267–271 (2004).
21. Tsutsui, M., Taniguchi, M. & Kawai, T. Local heating in metal-molecule-metal junctions. *Nano Lett.* **8,** 3293–3297 (2011).
22. Xiang, D. *et al.* Three-terminal single-molecule junctions formed by mechanically controllable break junctions with ide gating. *Nano Lett.* **13,** 2809–2813 (2013).
23. Huang, Z. *et al.* Local ionic and electron heating in single-molecule junctions. *Nat. Nanotechnol.* **2,** 698–703 (2007).
24. Todorov, T. N., Hoekstra, J. & Sutton, A. P. Current-induced embrittlement of atomic wires. *Phys. Rev. Lett.* **86,** 3606–3609 (2001).
25. Tsutsui, M. *et al.* Atomically controlled fabrications of subnanometer scale electrode gaps. *J. Appl. Phys.* **108,** 064312 (2010).
26. Tsutsui, M. Taniguchi, M. & Kawai, T. Atomistic mechanics and formation mechanism of metal-molecule-metal junctions. *Nano Lett.* **9,** 2433–2439 (2009).
27. Huisman, E. H. *et al.* Stabilizing single atom contacts by molecular bridge formation. *Nano Lett.* **8,** 3381–3385 (2008).
28. Ke, S.–H., Yang, W., Curtarolo, S. & Baranger, H. U. Thermopower of molecular junctions: An ab initio study. *Nano Lett.* **9,** 1011–1014 (2009).
29. Paulsson, M. & Datta, S. Thermoelectric effect in molecular electronics. *Phys. Rev. B* **67** 241403 (2003).
30. Mott, N. F. & Jones, H. The theory of the properties of metals and alloys. *(Oxford University Press, New York 1936)*.
31. Yee, S., Malen, J., Majumdar, A. & Segalman, R. A. Thermoelectricity in fullerene-metal heterojunctions. *Nano Lett.* **11,** 4089–4094 (2011).
32. Strange, M., Rostgaard, C., Hakkinen, H. & Thygesen, K. S. Self-consistent GW calculations of electronic transport in thiol- and amine-linked molecular junctions. *Phys. Rev. B* **83,** 115108 (2011).
33. French, W. R. *et al.* Atomistic simulations of highly conductive molecular transport junctions under realistic conditions. *Nanoscale* **5,** 3654–3659 (2013).
34. Szyja, B. M., Nguyen, H. C., Kosov, D. & Doltsinis, N. L. Conformation-dependent conductance through a molecular junction. *J. Mol. Model.* **19,** 4173–4180 (2013).
35. Surgueev, N., Tsetseris, L., Verga, K. & Pantelides, S. Configuration and conductance evolution of benzene-dithiol molecular junctions under elongation. *Phys. Rev. B* **82,** 079106 (2013).
36. Torres, A., Pontes, R. B., da Silva, A. J. R. & Fazzio, A. Tuning the thermoelectric properties of a single-molecule junction by mechanical stretching. *Phys. Chem. Chem. Phys.* **17,** 5386–5392 (2015).

Acknowledgements

This research was supported in part by Strategic Information and Communications R&D Promotion Programme (122107001) of Ministry of Internal Affairs and Communications, ImPACT Program of Council for Science, Technology, and Innovation (Cabinet Office, Government of Japan), and "Nanotechnology Platform Project (Nanotechnology Open Facilities in Osaka University)" of Ministry of Education, Culture, Sports, Science and Technology, Japan [No: F-12-OS-0016]. M. Tsutsui acknowledges support from Foundation Advanced Technology Institute, The Thermal & Electric Energy Technology Foundation,Kansai Research Foundation for technology promotion, Yazaki Memorial Foundation for Science andTechnology, The Program for Creating Future Wisdom (Osaka University, selected in 2014), and The Asahi Glass Foundation.

Author Contributions

M.T. and M.T. planned and designed experiments. M.T. and T.M. fabricated microheater-embedded MCBJs and conducted break junction measurements. M.T., T.M., and A.A. performed data analyses. Y.H. carried out finite element analyses. M.T. and M.T. co-wrote paper.

Additional Information

Supplementary information accompanies this paper at http://www.nature.com/srep

Competing financial interests: The authors declare no competing financial interests.

How to cite this article: Tsutsui, M. *et al.* High thermopower of mechanically stretched single-molecule junctions. *Sci. Rep.* **5**, 11519; doi: 10.1038/srep11519 (2015).